ANALYTICAL STUDY ABOUT THE EXPANSION PROGRESS OF CONCRETE EXPOSED TO COMBINED ALKALI SILICA REACTIONS AND FREEZING THAWING CYCLES

Yuya Takahashi (1), Fuyuan Gong (2) and Koichi Maekawa (3)

(1) Department of Civil Engineering, The University of Tokyo, Japan

(2) College of Civil Engineering and Architecture, Zhejiang University, China

(3) Department of Civil Engineering, Yokohama National University, Japan

Abstract

Using numerical simulations, this study investigated the concrete expansion damage caused by the coupled action of freeze-thaw cycles (FTC) and alkali silica reactions (ASR). In the authors' previous experiments, it was shown that a preceding ASR definitely accelerated the succeeding expansion by FTC. Further, even if the specimens have sufficient entrained air to prevent expansion by sole FTC action, they can expand under the combination of ASR and FTC. The presence of air voids in specimens has little effect on the single ASR expansion rates. These observed experimental trends were analyzed by numerical simulations. Authors have proposed the mixed pore pressure and concrete expansion models for coupled ASR and FTC, and a non-linear finite element system for concrete structures was used to analyze them. These models were used to work out the factors governing the experimental trends. By comparing the experiments and simulations, it appears the air voids contribution can be the key factor on the coupled ASR and FTC expansion process. With effective modeling of microscopic ASR-gel and ice formations inside air voids, the experimental trends can successfully be reproduced numerically.

Keywords: Combined deterioration, Alkali silica reaction, Freezing thawing cycles

1. INTRODUCTION

Concrete structures in service have to endure various environmental actions simultaneously and the deterioration process of concrete is highly complicated. For example, on road structures in colder regions, anti-freezing salt used to reduce freeze-thaw cycle (FTC) damage can accelerate expansion by alkali silica reaction (ASR) and additional damage. The deterioration process is not easily explained by a single deterioration mechanism, and is expressed more effectively as coupled action deterioration. Previous research [1,2] conducted combined FTC and ASR action experiments on concrete, and increased discussion of these detailed mechanisms is needed to predict future behavior of these complicated phenomena.

Authors [3] have been developing models that consider the combined FTC and ASR deterioration on concrete. This study focuses on the expansion progress of concrete under combined FTC and ASR and the characteristic behaviors observed in previous experiments [4] using the developed numerical models tried to be understood.

2. REFERENTIAL EXPERIMENT

In the authors' previous papers [4], a combined FTC and ASR experiment was conducted with different water-to-cement (W/C) ratios, air contents, and sequences of ASR/FTC actions. Table 1 presents the experimental series and mix proportions. Six concrete specimen series were prepared with two different target air contents (1% and 6%), and three different W/C ratios (35%, 50%, and 60%). Ordinary Portland cement was used. Fine aggregate is not reactive during ASR, while coarse aggregate acts as the reactive andesite. Sodium chloride was added to the specimens to accelerate ASR expansion and the total alkali content in terms of Na_2O_{eq} was 10.0 kg/m^3. Four series of deterioration processes (single FTC, single ASR, FTC after ASR, and ASR after FTC) were implemented and two 10×10×40 cm prism specimens were prepared for each case to measure expansion progress. After hardening the air contents and air bubble spacing coefficients were measured and those values are listed in Table 1. In the target 1% air content cases, the air content of fresh mortar was approximately 2% and subsequently became approximately 1% after hardening, leading to higher air bubble spacing coefficients. The target 6% air content cases have more than 6% air content in fresh mortar, but they decreased to less than 5% after hardening.

Figures 1 and 2 show the measured expansion progress of the specimens with the target 1% and 6% air contents, respectively [4]. The figure sequences, (i) – (iv) show the single FTC expansions, the ASR expansions after FTC, the single ASR expansions, and the FTC expansions after ASR, respectively. The length changes are plotted by considering a length of zero before each deterioration action, and the results of two specimens are expressed in the legend as xx-x-1 and xx-x-2.

Among the single FTC process cases (Figs. 1(i) and 2(i)), the expansion in the 35-6 case was minimal, which indicates high resistance against FTC action. The specimens with higher air contents and lower W/C were confirmed to have higher FTC resistance due to the entrained air resistance against FTC actions and ice pressures. For the single ASR acceleration process, the lower the W/C, the larger the expansion after 13 weeks of ASR

Table 1: Series of specimens and mix proportions [4]

	Air (%)	W/C (%)	W	C	S	G	NaCl	water-reducing agent	AE	Air of fresh mortar (%)	Slump (cm)	Air after curing (%)	bubble spacing coeff. (μm)
35-1	1	35	175	500	717	914	17.17	C×0.7%	20T	1.7	5.5	1.3	1156
50-1		50	175	350	836	999	18.87	C×1.0%	20T	2	6	0.9	1422
60-1		60	175	292	839	1044	19	C×1.0%	20T	1.9	4.1	0.8	1154
35-6	6	35	175	500	736	845	17.17	C×0.7%	4.0A	6.6	16.5	4.3	273
50-6		50	175	350	777	928	18.87	C×0.9%	6.0A	6.2	11.2	2.7	336
60-6		60	175	292	781	971	19	C×1.0%	8.5A	6.5	15.4	4.8	302

accelerations. Furthermore, no significant difference exists between the 1% and 6% air content cases. Entrained air is therefore considered as having little buffering contribution to expansion pressure caused by ASR.

Figures 1(iv) and 2(iv) show that all cases have rapid expansion. As mentioned earlier, minimal expansion occurred in the 35-6 case during the single FTC process; however, significant expansion occurred during the FTC after the ASR process. Even if the preceding ASR expansion is small, such as in the 60-6 case (Fig. 2(iii)), the subsequent FTC expansion after ASR (Fig. 2(iv)) occurs much faster than the single FTC (Fig. 2(i)). The preceding ASR did have an effect on the subsequent FTC progress. The effective ability of entrained air to resist FTC damage can be impaired by a preceding ASR. In the case of ASR after FTC, the expansion rates (Figs. 1(ii) and 2(ii)) showed no significant difference from that of a single ASR action case (Figs. 1(iii) and 2(iii)).

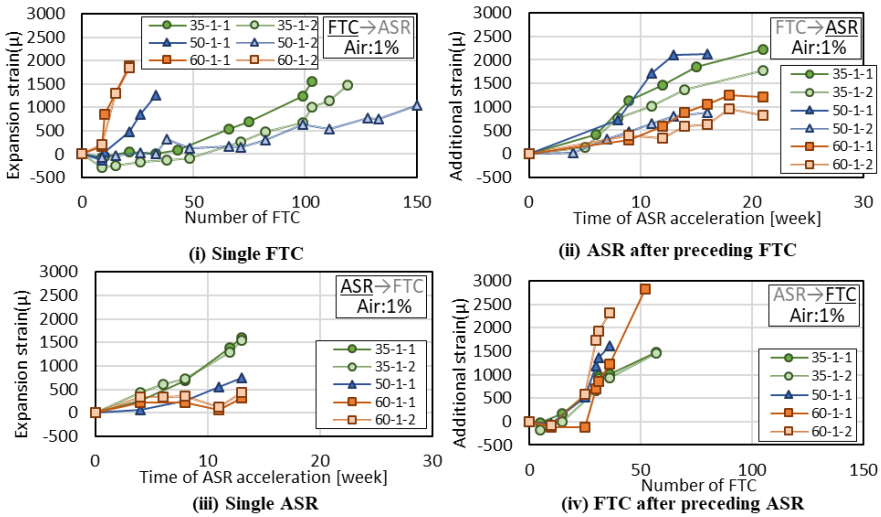

Figure 1: Sequential expansion of ASR and FTC for non-air entrained concrete [4]

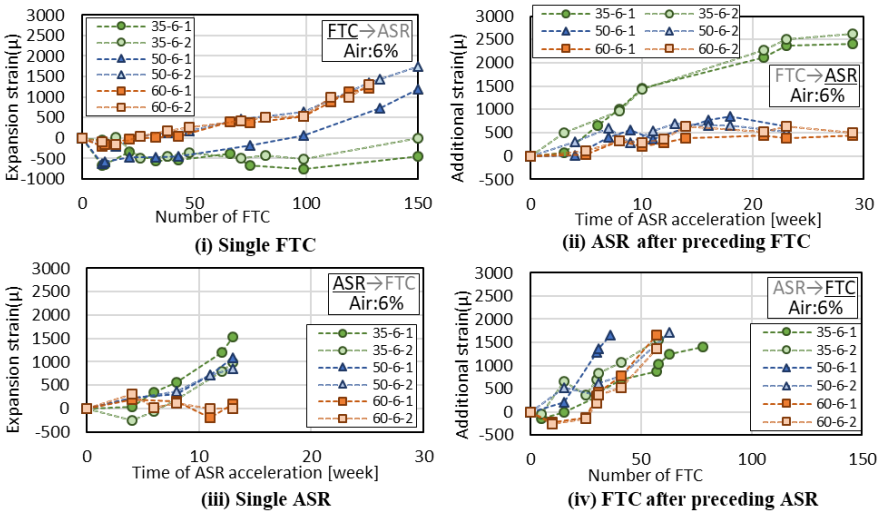

Figure 2: Sequential expansion of ASR and FTC for air entrained concrete [4]

3. PORO-MECHANICAL SIMULATION MODELS

The authors have been developing an analytical scheme to simulate concrete deterioration by combined FTC and ASR actions [3]. The models considering the internal pressures and deformations of ASR gel and ice inside cracks or voids are formulated based on the poro-mechanics, and they are implemented in the multi-scale chemo-hygral analytical scheme named DuCOM-COM3 [5]. The formulation details can be referenced in the previous paper [3]. The volume formulations of ASR gel and ice are summarized as follows:

The effective ASR gel volume (V_{ASR}) and ice expansion volume (V_{ICE}) that can contribute to the poro-mechanical expansion are expressed as Eqs. (1) and (2) [3].

$$V_{ASR} = V_{ASR\_TOTAL} - (S_{ASR} + V_{ASR \rightarrow AIR}) \quad (1)$$

$$V_{ICE} = 0.09 S_{ICE} - max\,(0.1 Air - V_{ASR \rightarrow AIR}, 0.0) \quad (2)$$

where V_{ASR_TOTAL} is the total created ASR gel volume formulated as a function of the alkali concentration, updated free water, and the reactive aggregate content [6], S_{ASR} and S_{ICE} are the volume of spaces occupied by ASR-gel and ice in the pore sized cement paste distribution, respectively, as shown in Fig. 3, and Air is concrete air content. $V_{ASR \rightarrow AIR}$ is the ASR gel volume absorbed to air bubbles and is formulated as follows:

$$\dot{V}_{ASR \rightarrow AIR} = k_{AIR} \cdot (1.0 - \beta_{ASR \rightarrow AIR}) \cdot p_{ASR} \cdot Air \quad (3)$$

where k_{AIR} is a constant determining the gel intrusion speed to air bubbles, $\beta_{ASR \rightarrow AIR} = (V_{ASR \rightarrow AIR}/Air)$ is the ASR gel occupying ratio in the air bubbles (0.0-1.0) and p_{ASR} is the ASR gel pressure. As formulated in Eq. (1), some created ASR gel potions can be absorbed in capillary pores (equivalent to S_{ASR}) and air bubbles (equivalent to $V_{ASR \rightarrow AIR}$) and they do not contribute to the ASR expansion. Ten percent of existing air bubbles and capillary pores larger than the minimum freezing radius (r_{ICE}) excluding inkbottle pores (S_{ink}) are available for ice formation, except the space pre-occupied by ASR-gel (S_{ASR} and $V_{ASR \rightarrow AIR}$). The k_{AIR} value is provisionally set as 2.0E-9 $Pa^{-1}s^{-1}$ in the previous study, but the proper value is discussed in the following chapter.

V_{ASR} and V_{ICE} are considered in the dynamic equilibrium equations of the concrete skeleton and each pore substance in cracks and the concrete expansion can be calculated.

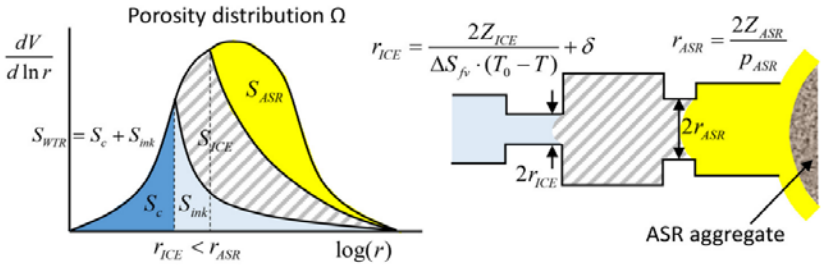

Figure 3: ASR gel intrusion and ice formation in pores [3]

4. ANALYTICAL STUDIES

4.1 Single ASR cases

Using the previous chapter's summarized analytical scheme, simulation of the reference experiments [3,4] was attempted. Prism-shaped meshes of 10-10-40 cm are prepared and the

same mix proportions, curing conditions, and environmental conditions are entered. The simulated single ASR case results are shown in Fig. 4.

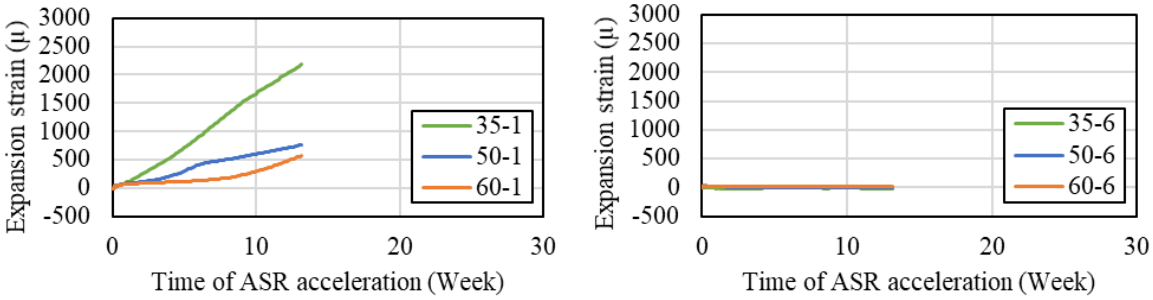

(i) Air 1% cases (ii) Air 6% cases

Figure 4: Simulated expansion progresses for single ASR cases (k_{air}=2.0E-9)

It can be observed in Fig. 4 that the 1% air cases agree well with the experiments (Fig. 1(iii)), while no expansion occurs in all 6% air cases. The calculated V_{ASR}, V_{ASR_TOTAL} and (S_{ASR}+$V_{ASR\rightarrow AIR}$) for the 50-6 case are plotted in Fig. 5. Here, not only in the k_{AIR} = 2.0E-9 case (Fig. 5(i)), but also for the k_{AIR} = 5.0E-9 and 1.0E-10 cases are simulated and plotted. All generated ASR gels are absorbed to air bubbles and capillary pores in the k_{AIR} = 2.0E-9 case, but lower k_{AIR} values reduces the gel absorption to voids and increases the effective ASR gel volumes. Figure 6 shows the expansion progress of the 50-6 case under various k_{AIR} values, and shows that the expansion progress corresponds to V_{ASR} increases. With a low enough value (k_{AIR} =1.0E-10), the calculations for 6% air cases were conducted again (Fig. 7) and the simulations properly reproduce the experimental trends (Fig. 2(iii)). The ASR gel intrusion behavior into voids is influential in the ASR expansion progress calculations.

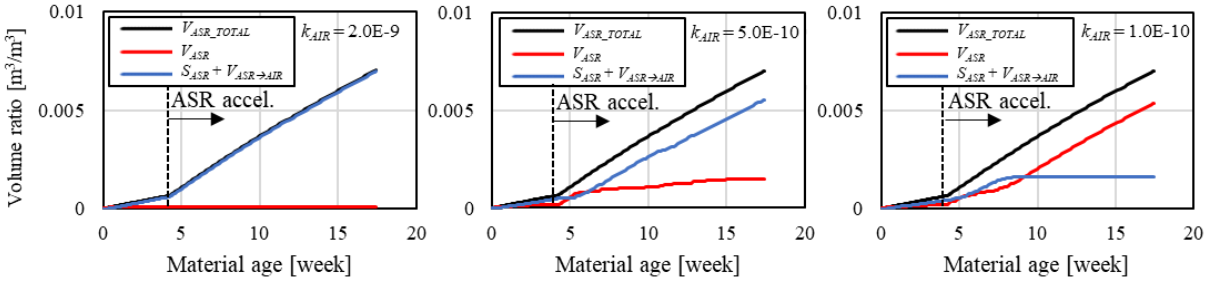

(i) k_{AIR} = 2.0E-9 (ii) k_{AIR} = 5.0E-10 (iii) k_{AIR} = 1.0E-10

Figure 5: ASR gel volumes simulated in 50-6 case with different k_{AIR} values

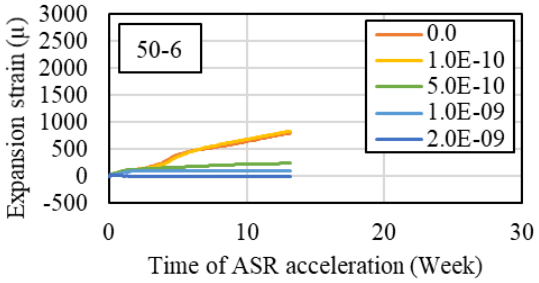

Figure 6 : Expansion progress of 50-6 case with various k_{AIR} values

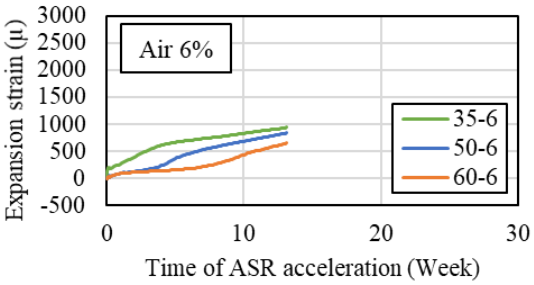

Figure 7 : Expansion progress for single ASR cases with k_{AIR} = 1.0E-10

4.2 Single FTC case

The air content and air bubble size distributions after hardening are quite influential parameters in the FTC deterioration processes, and it is difficult to control them precisely as designed (as shown in Table 1). This is one reason for the large data scattering in FTC deterioration experiments. In both the model and simulations, results can differ greatly due to entered air content, and proper air content values should be determined to reproduce each experimental result. For this study's reference experiments, the values are determined by sensitivity analyses of input air contents; 2.0%, 2.6%, 1.0%, 6.0%, 4.2% and 4.95% can be proper air content values for 35-1, 50-1, 60-1, 35-6, 50-6, 60-6 cases, respectively. The simulated single FTC action expansion progress with determined input air contents are shown in Fig. 8.

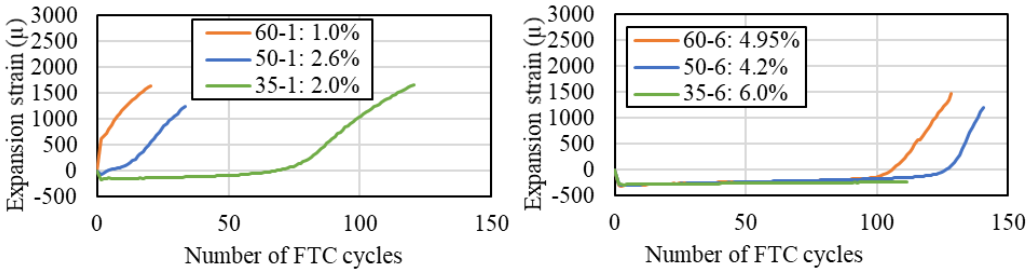

(i) Air 1% cases (ii) Air 6% cases

Figure 8: Expansion progress for single FTC actions

With appropriate input air content values, the resistivity differences between FTC actions can be reproduced. The frost damage resistivity should be determined not only by air content, but also by air bubble size distribution (or air bubble spacing factors). Future investigations should seek integrated ways to input resistivity against frost damage appropriately, considering bubble size distribution. The determined input air content values here are used in the following study simulations as the provisional values.

4.3 Combined FTC and ASR cases

In the reference experiment, the subsequent FTC expansions are accelerated even if the preceding ASR expansion is quite small, as seen in the 60-6 case (Fig. 2). This could mean that ASR gel can be intruded to entrained air even if there is little expansion, and impairs the effective ability of the entrained air to resist FTC damage. Here, $V_{ASR \rightarrow AIR}$ should be a critical factor governing the expansion progress and accordingly the effect of k_{AIR} is investigated for the ASR → FTC case.

The simulations of preceding ASR expansion and subsequent FTC expansion for the 50-6 case are conducted with different values of k_{AIR}, i.e., 1.0E-9, 5.0E-10 and 1.0E-10. Figure 9 shows the calculated volume graphs of ASR gels during ASR acceleration, and expansion progresses during preceding ASR and succeeding FTC actions. As mentioned in the previous section, inputted air content is 4.2%, expressing the proper frost damage resistance of the experiments.

With larger values of k_{AIR} such as 1.0E-9 (Fig. 9(i)), subsequent FTC expansion is accelerated compared to the single FTC case (Fig. 8). This is because the air bubbles are occupied by ASR gels, while there is little expansion during the preceding ASR period because most portions of generated ASR gels are absorbed to the air voids and capillary pores.

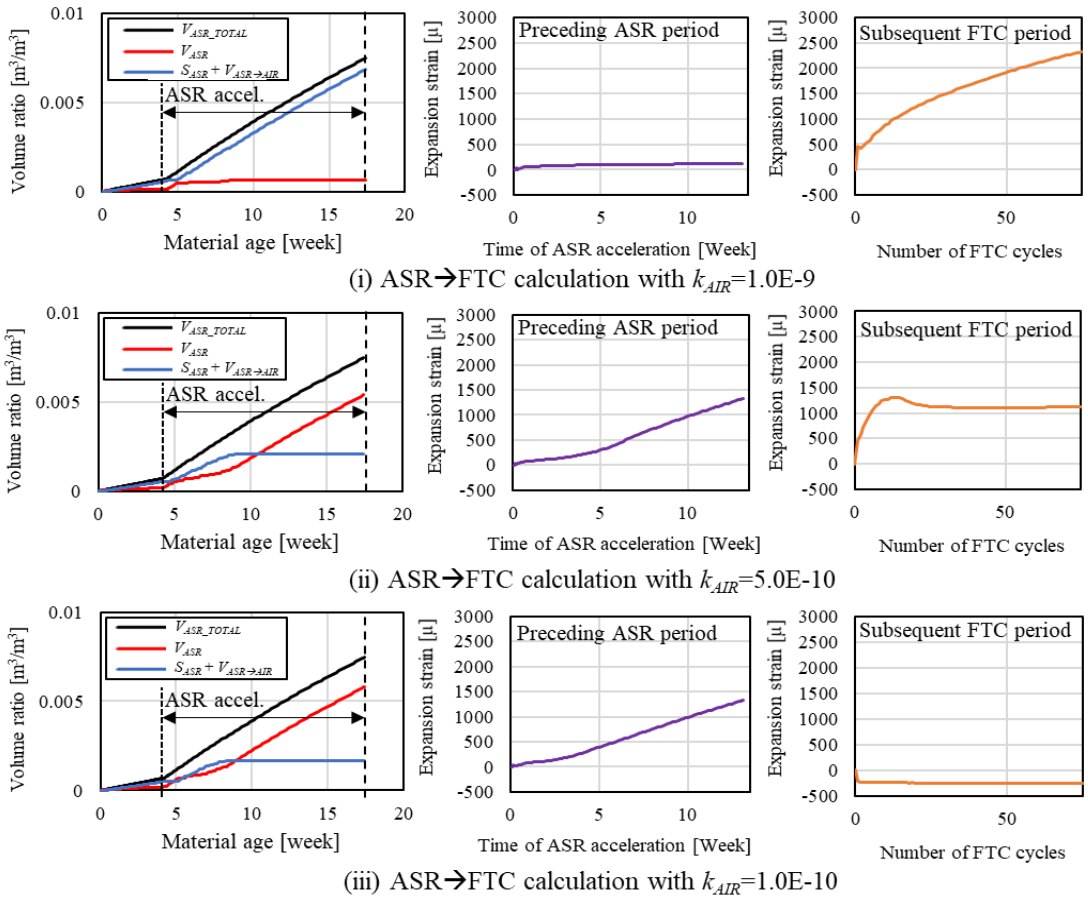

Figure 9 : Simulated results for ASR → FTC actions of 50-6 case

On the other hand, with smaller values of k_{AIR} such as 1.0E-10 (Fig. 9(iii)), expansion occurs during the ASR acceleration period due to less gel absorption to air and pores, but the smaller occupation of air voids by ASR-gel fails to accelerate the subsequent expansion by FTC actions. Only with the intermediate value such as k_{AIR} = 5.0E-10, expansion occurs during the ASR acceleration period and acceleration of subsequent FTC expansions can also be observed. It is understood that the time-dependent multiphase behavior inside air bubbles is important in realizing the expansion behavior during combined effects of FTC and ASR on concrete. With the determined value of k_{AIR} (5.0E-10), 6% air cases are simulated, and the results are shown in Fig. 10. With all air contents, the subsequent FTC expansions are accelerated compared to the single FTC case (Fig. 8(ii)), while the expansion rate of subsequent FTC differs from experimental results (Fig. 2(iv)). Also, k_{AIR} = 5.0E-10 still seems larger for the 35-6 case because there is no expansion in the preceding ASR acceleration period.

The role of air voids in concrete for the combined actions of FTC and ASR is realized in this study. However, it is still difficult to predict all experimental results with the limited factors appearing in this study. Further model investigations should be completed for combined ASR and FTC actions based on the microscopic multiphase phenomena inside air bubbles. The FTC → ASR case is even more difficult to predict. Figure 11 shows the succeeding ASR expansion of 6% air cases simulated after the FTC deteriorations shown in Fig. 8 (ii). The succeeding ASR is affected by preceding FTC in simulations, while little experimental influence is seen. The mechanisms responsible for the small effect of FTC on ASR progress should be studied.

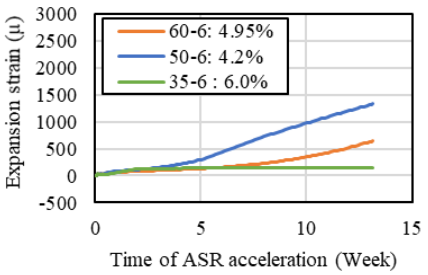

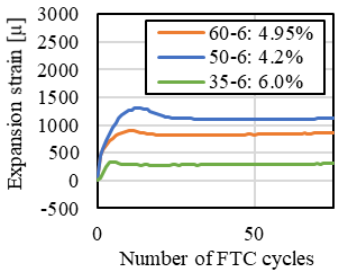

Figure 10: Simulation results for ASR → FTC actions for air 6% case (k_{AIR} =5.0E-10)

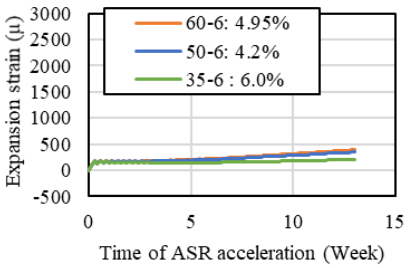

Figure 11: FTC → ASR simulations for air 6%

5. CONCLUSIONS

This study investigates the process of concrete expansion damage by the coupled actions of FTC and ASR focusing on the role of air bubbles in the concrete. Based on the poro-mechanical models, the referenced experiments of the combined FTC and ASR effects were attempted by simulation. In the single ASR action simulations, it is realized that enough low ASR-gel absorption rate to air bubbles should be considered to predict the expansion progress of high air entrained concrete accurately. In the coupled ASR and FTC simulations, the intermediate rate of gel absorption to air allows both the maintaining of preceding ASR expansions higher and the subsequent acceleration of FTC expansion. The detailed multiphase behavior inside air bubbles during coupled FTC and ASR actions is needed for quantitative prediction of deterioration behavior caused by these coupled actions.

ACKNOWLEDGEMENTS

This study was financially supported by the National Key R&D Program of China (2017YFC0806100), the Fundamental Research Funds for the Central Universities (2019QNA4032) and JSPS KAKENHI grant number 18H01507.

REFERENCES

[1] Bérubé, M., Chouinard, D., Pigeon, M., Frenette, J., Boivert, L. and Rivest, M. 'Effectiveness of Sealers in Counteracting Alkali-silica Reaction in Plain and Air-Entrained Laboratory Concretes Exposed to Wetting and Drying, Freezing and Thawing, and Salt Water', *Canadian Journal of Civil Engineering*, **29** (2002) 289-300.

[2] Deshenes, R.A., Giannini, E.R., Drimalas, T., Fournier, B. and Micah Hale, W. 'Effects of Moisture, Temperature, and Freezing and Thawing on Alkali-Silica Reaction', *ACI Materials Journal*, **115**(4) (2018) 575-584.

[3] Gong, F., Takahashi, Y. and Maekawa, K. 'Multi-scale computational modeling for concrete damage by mixed pore pressures -case of coupled alkali-silica reaction and cyclic freeze/thaw', *Engineering Computations*, **35**(6) (2018) 2367-2385.

[4] Segawa, I., Takahashi, Y., Gong, F. and Maekawa, K. 'Expansions and damage processes of concrete due to coupled alkali silica reactions and freeze-thaw cycles', In: Proceedings of the 8th International Conference of Asian Concrete Federation, 2018, 649-658.

[5] Maekawa, K., Ishida, T. and Kishi, T. 'Multi-Scale Modeling of Structural Concrete', Taylor and Francis, 2008.

[6] Takahashi, Y., Ogawa, S., Tanaka, Y. and Maekawa, K. 'Scale-Dependent ASR expansion of concrete and its prediction coupled with silica gel generation and migration, *Journal of Advanced Concrete Technology*, **14**(8) (2016) 444-463.